ACS NANO

www.acsnano.org

ARTICLE

Stretchable Biaxial and Shear Strain Sensors Using Diffractive Structural Colors

Ying-Jun Quan, Young-Gyun Kim, Min-Soo Kim, Soo-Hong Min, and Sung-Hoon Ahn*

Cite This: *ACS Nano* 2020, 14, 5392–5399

Read Online

ACCESS | Metrics & More | Article Recommendations | Supporting Information

ABSTRACT: Structural colors that can be changed dynamically, using either plasmonic nanostructures or photonic crystals, are rapidly emerging research areas for stretchable sensors. Despite the wide applications of various techniques to achieve strain-responsive structural colors, important factors in the feasibility of strain sensors—such as their sensing mechanism, stability, and reproducibility—have not yet been explored. Here, we introduce a stretchable, diffractive, color-based wireless strain sensor that can measure strain using the entire visible spectrum, based on an array of cone-shaped nanostructures on the surface of an elastomeric substrate. By stretching or compressing the substrate, the diffractive color can be tuned according to the changing grating pitch. Using the proposed method, we designed three types of strain-sensing modes: large-deformation (maximum 100%) tensile strain, biaxial 2D strain, and shear strain (maximum 78%). The strain sensors were fabricated, and applicability to strain-sensing was evaluated.

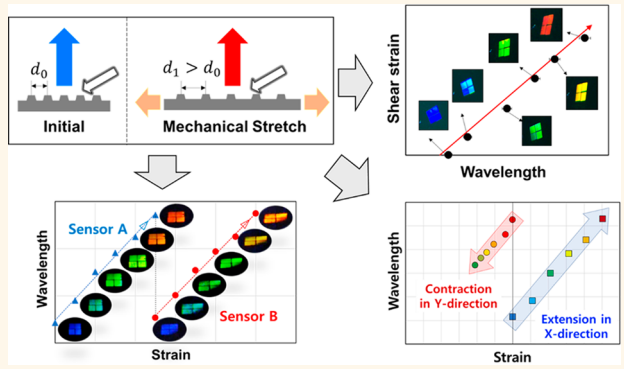

KEYWORDS: *structural color, strain sensor, diffractive color, full-color change, stretchable, shear strain sensor*

Due to the increasing demand for sensors in recent various fields, research has been conducted toward the development of strain sensors for human motion detection, soft robotics, and human−machine interfaces.[1−5] However, narrow measurable ranges and wired connections to external data acquisition equipment have remained as technological obstacles for actual usage.[6−9] Structural color, in particular, as generated by micro/nanoperiodic structures, has recently become an important research topic.[10−24] Because of the advantages of chemical stability, vivid coloration, and anti-discoloration, structural color has been reported in applications such as color printing,[25,26] color filters,[27−29] and sensors.[14,30,31]

Recently, wireless strain sensors capable of exploiting structural colors have attracted interest for the monitoring of the structural integrity in soft robotics. Many approaches for mechanically tuning color using photonic crystals and plasmonic nanostructures have been reported.[13,17,19,32−36] However, only the color change mechanism based on mechanical deformation, and its potential application to strain sensors, has been described thus far. The feasibility for such strain sensors has not been demonstrated in terms of their strain-sensing mechanism, reproducibility, and repeatability.

Two techniques are typically used to fabricate soft, mechanically color-tunable devices. One is self-assembly, which uses a chemical technique to produce nanoparticle arrays in soft elastomers,[36] and the other is soft lithography, which fabricates metallic nanopatterns that create structural colors on the surfaces of elastomeric materials,[19] However, both processes require complex equipment and procedures, which results in a high manufacturing cost.

In this study, we focused on implementable and interoperable strain sensors, based on structural coloration with a large measurable range and with the advantages of wireless detection and low cost due to a simple manufacturing process. We experimentally showed the full visible color-based strain sensor and using theoretical calculation to model the relationship between strain and color spectrum, which can be further used in large deformable applications. A mechanically tunable diffractive color structure is proposed using a focused ion beam (FIB)[37] and modified thermal nanoimprinting process. A two-dimensional (2-D) nanopattern of cone shape is designed on the surface of an elastomeric material. The elastomeric

Received: November 11, 2019
Accepted: April 10, 2020
Published: April 10, 2020

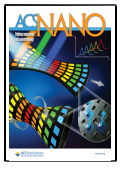

https://dx.doi.org/10.1021/acsnano.9b08953
ACS Nano 2020, 14, 5392−5399

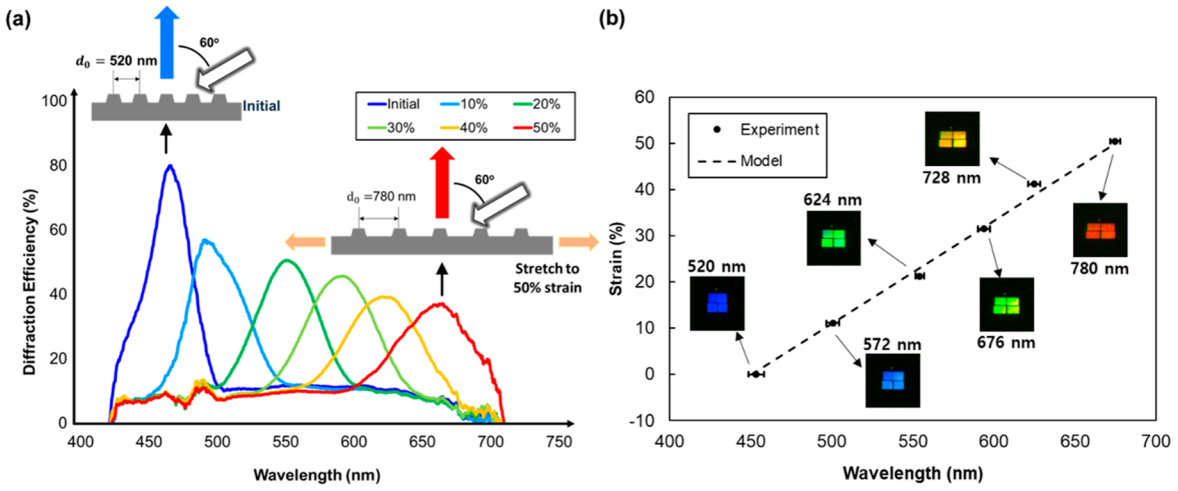

Figure 1. Working principle of our full-spectrum diffractive color-based strain sensor. (a) Schematic diagram of the stretchable diffractive color-based strain sensor, with experimental results for diffracted wavelength on stretching from 0% to 50%. The diffraction efficiency of color-based strain sensor measured in this research is approximately from 40% to 80% during tensile stain. (b) Charge-coupled device (CCD) images of the reflected colors and comparison of experimental results to a theoretical model of the strain spectra of our diffractive color-based strain sensor.

material that we used in this research, namely, polydimethylsiloxane (PDMS), has been widely used in stretchable technologies because it is nontoxic, nonflammable, and highly stretchable. With a different diffraction pattern design, the proposed color-based strain sensor can measure large uniaxial tensile strain (ε = 100%), 2-D biaxial strain, and shear strain (γ = 78%), all within the visible spectrum. The wireless and low-cost color-tunable strain sensor developed here is expected to create further opportunities for smart and flexible manufacturing.

RESULTS AND DISCUSSION

In this research, we developed a diffractive structural color-based strain sensor that can measure tension, compression, and shear using various designed patterns. The concept of our color-based strain sensor is shown in Figure 1. To achieve full color shifts without approaching the elastic limit of the elastomer, the strain sensor is designed to measure strain from 0% to 50% based on full-color images (from blue to red). The sensor is designed to show a blue color in its relaxed state, which has a pattern pitch of 520 nm. Blue light is reflected along the normal direction under the relaxed state, when white light is incident from a given angle. When the substrate is stretched, the interspacing of the diffraction pattern increases, and the color shifts from blue to red (Figure 1a). The diffraction spectrum is highly sensitive to grating pitch, and the color can be changed to any visible color.

With white light irradiation, the factors affecting diffractive coloration include the grating pitch, Λ, and the angles of incident light, α, and reflected light, β, and the diffracted wavelength, λ, in the mth order. The relationship between Λ and λ is given by eq 1. In this paper, the angles of incidence and reflection are given as 60° and 0°, respectively.

$$m\lambda = \Lambda(\sin\alpha - \sin\beta) \quad (1)$$

From the diffraction equation, eq 1, for a given configuration of incident and reflected angles, the diffraction spectrum can be determined by the pattern period. Because the diffraction spectrum is only related to the period of the periodic nanopattern, a color change can be achieved by stretching the nanopatterned elastomers, thereby increasing the grating pitch. Thus, the normal strain can be measured by measuring the diffraction spectrum. To utilize the proposed structures as a strain sensor, the correlation between strain, ε, and diffraction wavelength, λ, is required. The relationship of diffraction wavelength to strain is obtained by deriving the diffraction equation (see Supporting Information section 2):

$$\varepsilon = 0.2221\lambda - 100 \quad (2)$$

Diffraction spectra of the color-based strain sensor were measured using a self-built optical system. Supporting Information Figure S1 shows a schematic diagram of the optical setup for measuring diffractive colors and diffraction spectra. The diffraction spectra under different strain conditions were collected with an objective lens in reflection mode and captured with a dark-field charge-coupled device (CCD). The spectra and images were observed along the normal direction (Figure 1a). The wavelength of the maximum peak of reflected color is changed from 457 nm to 665 nm by stretching the sensor from its relaxed state to 50% mechanical strain. The intensity of the peak wavelength is decreased by increasing the strain. By stretching the sensor, the height of the nanotip structure is decreased due to Poisson's ratio. Therefore, the intensity of the reflected light is also decreased.[38] The diffraction efficiency of the nanostructure measured at its original status, which is a blue color, is approximately 80%. The diffraction efficiency is decreased from 80% to approximately 40% by stretching the sensor, which is because of the height decrease of the nanopillar structure.

The results of our experiments, a theoretical model of the strain spectra of our diffractive color-based strain sensor, and color images under different strains are shown in the CCD images of Figure 1b; the sensor shows a blue color in the relaxed state. By increasing the strain from 0% to 50% in 10% steps, the color of the sensor changed to light blue (ε = 10%), green (20%), light green (30%), orange (40%), and red (50%). Corresponding to the color change, the average wavelength of the peak reflection shifted from 453 nm to 675 nm. We

https://dx.doi.org/10.1021/acsnano.9b08953
ACS Nano 2020, 14, 5392−5399

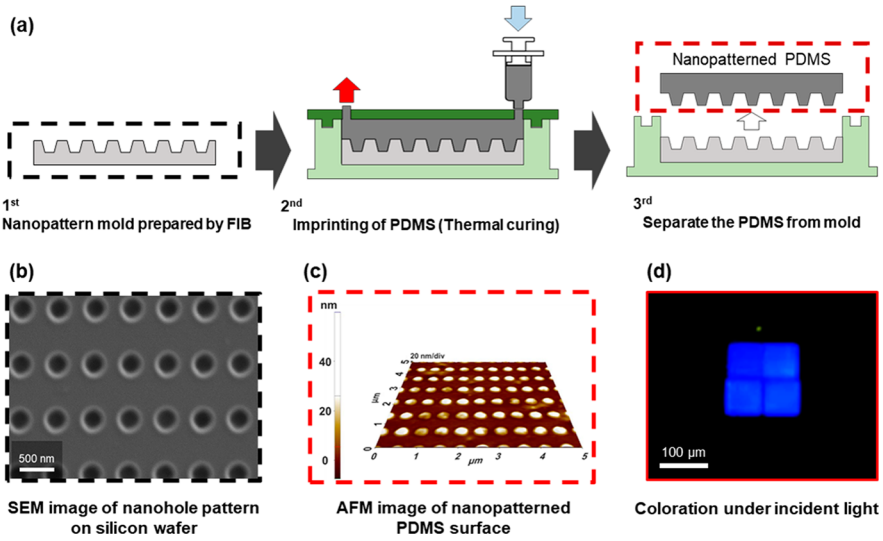

Figure 2. Fabrication process of the structural color-based strain sensor. (a) Schematic diagram of sample fabrication. The diffracting pattern mold was fabricated by a FIB nanomilling process on the silicon substrate. The nanopattern mold was placed into the sample mold, and polydimethylsiloxane (PDMS) was thermally imprinted. The surface nanopatterned PDMS sample was peeled off from the mold after curing. (b) SEM image of the nanohole patterned mold and (c) AFM image of a nanopattern on the PDMS surface. (d) Optical microscope image of a surface nanopatterned PDMS sample under white incident light with a pattern distance of 520 nm.

compared our experimental results with a theoretical model of strain spectra that we also designed. The experimental results substantially agree with the theoretical model.

The diffractive color-based strain sensor was fabricated using a thermal nanoimprinting process. Initially, a 2-D diffracting nanohole pattern was fabricated on a silicon substrate using a FIB nanomilling process. For large areas of such diffracting nanostructures, several other fabrication techniques can be used, such as photolithography. A scanning electron microscope image of the fabricated nanohole pattern on its silicon substrate is shown in Figure 2b. The nanohole pattern array size was 150 μm × 150 μm. A PDMS solution mixed with black pigment was prepared for the imprinting process. A modified thermal imprinting process was carried out to transfer the diffraction nanopattern from the silicon substrate to the surface of the PDMS substrate. The reason for using black silicone pigment with the PDMS is to prevent light scattering, which affects the diffractive color (see Figure S3). After curing, the surface-nanopatterned PDMS substrate was peeled from the mold (Figure 2a), and a diffraction nanopattern of corn shapes on a PDMS substrate was thus fabricated. In a typical experiment, the relaxed state is designed to present a diffractive blue color for a grating pitch of 520 nm. Figure 2c shows an atomic force microscope image of a fabricated sample. CCD images of the diffractive colors under our chosen illumination conditions are shown in Figure 2d. To confirm the elastic limit of the silicone–pigment mixed PDMS substrate, we conducted tensile tests of it with different weight ratios of pigment to PDMS (see Figure S4).

It is important to evaluate the repeatability and stability of our developed stretchable diffracting nanostructures for use as a strain sensor. Therefore, the process was repeated 1000 times and the reflection spectra were measured. The first, 100th, 500th, and 1000th relaxed and 50% strained spectra were measured, as shown in Figure 3. The color change induced by mechanical strain is highly reversible. Unlike plasmonic or photonic crystals, which are constructed of multiple materials, the developed diffractive sensor is a one-body structure

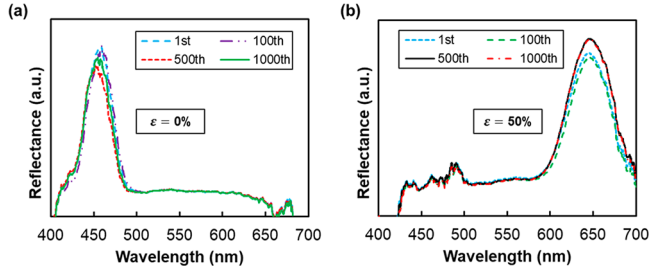

Figure 3. Experimental spectra of repeated tests: (a) relaxed state, (b) strain at 50%. The process was repeated 1000 times, and the 1st, 100th, 500th, and 1000th spectra were measured.

comprised of elastomer alone. The positions of the nanotip structure do not shift during deformation, and the material is below its elastic limit. The peak wavelengths for both initial and 50% strain vary very slightly, with standard deviations of ±3.35 nm and ±0.68 nm, respectively. Also, the thermal effect on the strain sensor was evaluated for different temperatures. Considering the fabricated strain sensor is not intended for use in a high-temperature environment, the spectra of diffraction nanopatterns with 520 and 780 nm spacing—which generate blue and red colors, respectively—were measured, and CCD images of the diffractive colors were acquired at temperatures ranging from 20 to 70 °C (Figure 4). The experimental results were compared with a theoretical model, which was calculated for a thermal expansion coefficient of 3.2 × 10^{-4}/°C.[39] The peak wavelength is slightly lower than the theoretical model, likely due to the inaccuracy of the thermal expansion coefficient of silicone–pigment mixed PDMS. In addition, the strain sensitivities under strain from 0% to 50% in terms of the temperature changes were tested to evaluate the performance of the strain sensor. The strain sensitivity (gauge factor) was defined by

$$\text{Gauge Factor (GF)} = (\Delta\lambda/\lambda_0)(1/\varepsilon) \quad (3)$$

where $\Delta\lambda/\lambda_0$ is wavelength change by mechanical strain. The results of strain sensitivity in terms of temperature changes are

https://dx.doi.org/10.1021/acsnano.9b08953
ACS Nano 2020, 14, 5392–5399

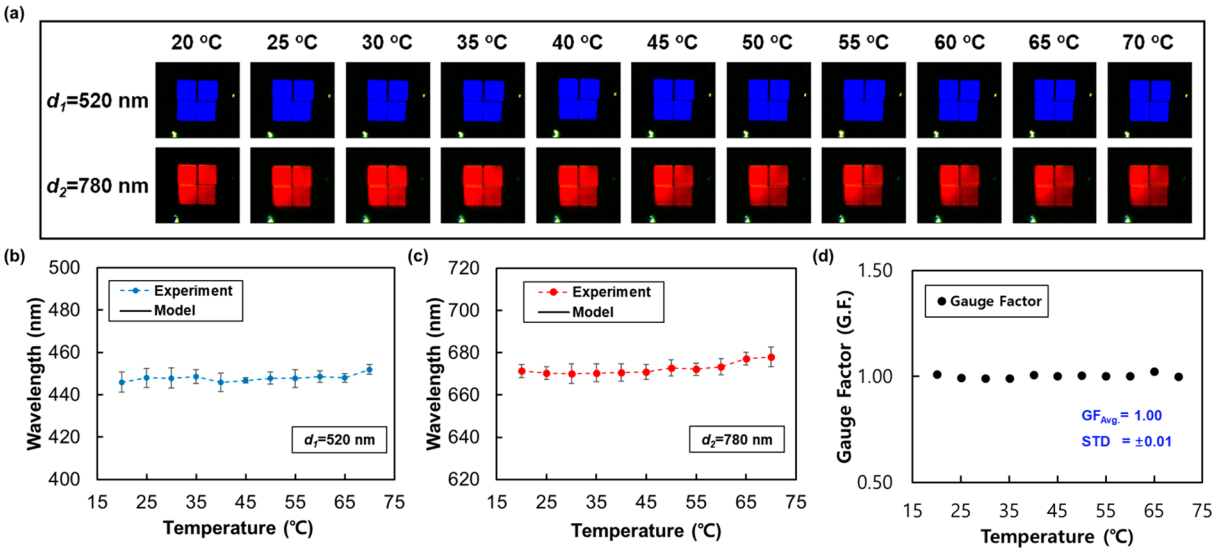

Figure 4. Effect of temperature on strain sensor. (a) CCD image of diffracted colors with pattern distances of 520 and 780 nm at temperatures ranging from 20 to 70 °C. The maximum spectral peak is compared with a theoretical model for (b) 520 nm (blue) and (c) 780 nm (red) pattern distances. (d) Sensitivity of the strain sensor at temperatures ranging from 20 to 70 °C.

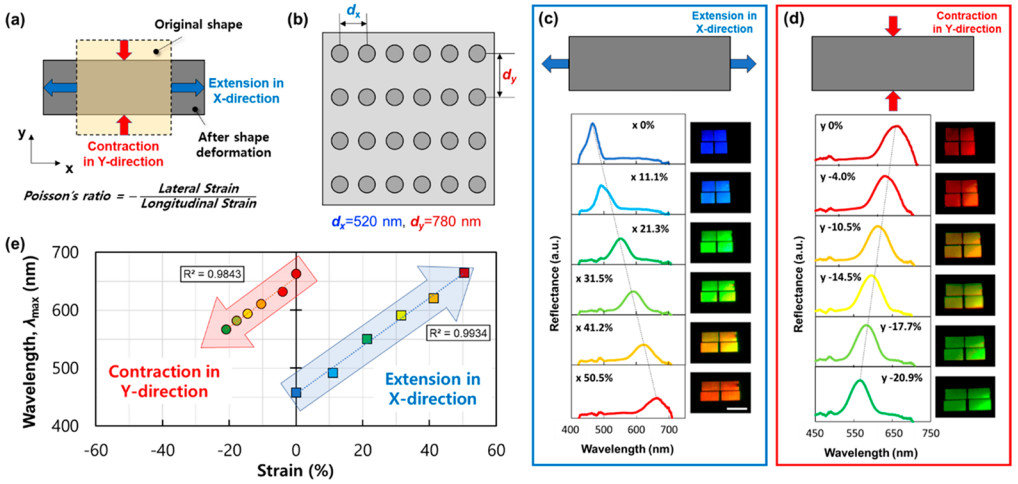

Figure 5. Biaxial strain sensor. (a) Schematic of Poisson's ratio and (b) diffraction pattern design for the biaxial strain sensor. (c) Images of expansion in the *x*-direction and the color spectra and (d) color images of contraction in the *y*-direction caused by Poisson's ratio. (e) Experimental results of the relationship between strain and spectrum for our two-dimensional strain sensor.

shown in Figure 4d. The calculated GFs under temperatures ranging from 20 to 70 °C are from 0.99 to 1.02, and the average GF is 1.00 with a standard deviation of ±0.01. The sensitivity of this strain sensor is almost changeless along with the increase of temperature, while the electrical resistance-based strain sensor responds sensitively to temperature changes.[40] The fabricated structural color-based strain sensor exhibits reliable and stable strain sensing performance under different temperature conditions.

Strain Sensor Design. *Biaxial Strain Sensor.* In solid mechanics, Poisson's ratio is an important factor when evaluating material properties. To evaluate material properties, we designed a 2-D biaxial, color-based strain sensor with different diffraction grating pitch in the horizontal and vertical directions. Most materials, including metals, plastics, and elastomers, have a negative Poisson's ratio, such that a material deformed in the horizontal direction will contract in the vertical direction (Figure 5a). Thus, we designed an asymmetric 2-D diffraction nanopattern, with a grating pitch of 520 nm along the *x*-axis and 780 nm along the *y*-axis, to obtain the initial status of the strain sensor (Figure 5b). The color will shift from blue to red when the material is stretched in the *x*-direction, and from red to blue in the *y*-direction because of Poisson's ratio. To confirm the color shift in both directions, the sample was stretched in the *x*-direction to 50% strain. The reflection spectrum with incident light in the *x*-direction is changed from a maximum peak at 442 nm (blue) to a peak at 665 nm (red) (Figure 5c). At the same time, the reflection spectrum with incident light in the *y*-direction is changed from 663 nm (red) to 567 nm (green) due to contraction (Figure 5d). The diffraction efficiency measured in the *y*-direction ranges from 73% to 80% (Figure S8). The relationship between strain and wavelength for the 2-D strain sensor is shown in Figure 5e. In this case, the Poisson's ratio of PDMS obtained from the measured spectrum is 0.410, while the actual value for the sample is 0.416. The standard error is nominally 1.12%, which is in the range of allowable error.

https://dx.doi.org/10.1021/acsnano.9b08953
ACS Nano 2020, 14, 5392−5399

100% Tensile Strain Sensor. Theoretically, the proposed diffractive structural colors can only cover a strain value up to 50% according to the range of the visible spectrum. To obtain a larger measurement range using this technique, our strain sensor combined two different diffraction nanopatterns that can measure tensile strain up to 100%. The working principle of the 100% strain sensor is shown in Figure 6a. The sensor

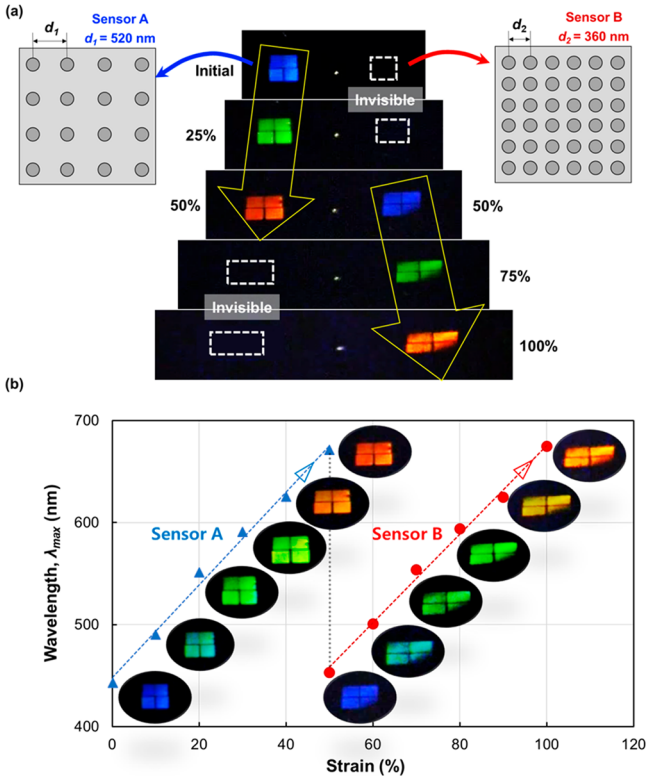

Figure 6. 100% strain sensor with two different diffraction patterns. (a) Working principle and CCD images of color change under 100% tensile strain. The sensor consists of two different nanopatterns, A and B, which have pattern distances of 520 and 780 nm, respectively. (b) Maximum spectral peak corresponding to tensile strain up to 100%.

consists of two diffraction nanopatterns, A and B. Pattern A has a grating pitch of 520 nm and can measure strain from 0% to 50%, while pattern B has a grating pitch of 360 nm, for measuring strain from 50% to 100%. When the sample is stretched up to 50%, the color of pattern A changes from blue to red. When the sensor is stretched to 50%, the grating pitch of pattern B is increased to 520 nm, which is the initial grating pitch of pattern A. Thus, the color of pattern B shifts from blue to red for a strain range from 50% to 100%. To demonstrate this principle, a strain sensor consisting of these two diffracting patterns was fabricated and stretched to 100% strain. As shown in Figure 6a, when the sensor is illuminated with a white light source in its relaxed state, the color is blue for pattern A, while pattern B is invisible; only when the sensor was stretched by 50% could the color of pattern B be observed (as blue). From 50% strain, the color of pattern B started to shift from blue to red, to cover the 50% to 100% strain range. Figure 6b shows the results of the maximum spectral peak corresponding to 100% tensile strain. Corresponding to the color shift, the maximum diffraction peak of the sensor shifted from 445 to 672 nm for pattern A and from 453 to 675 nm for pattern B.

Shear Strain Sensor. In solid mechanics, strains are classified as either normal or shear. A shear strain is parallel to the face of an element. Herein, we introduce a diffractive color-based shear strain sensor that can measure the simple shear strain in a plane. For a given square, by applying simple stress, the square will be elongated along the direction of a diagonal line, as shown in Figure 7a. Thus, we designed a diffraction nanopattern on the surface of the sensor, perpendicular to the diagonal of the square. The working principle of the shear strain sensor is shown in Figure 7a. Similar to a normal strain sensor, when a simple shear stress is applied to the sample, the reflected color will shift from blue to red by increasing the grating pitch along the diagonal direction.

To verify the concept of our diffractive color-based shear strain sensor, a theoretical model was developed according to a normal strain spectrum model (eq 2). The relationship of shear strain to wavelength is as follows (see Supporting Information section 5):

$$\gamma = 0.39\lambda - 172 \tag{4}$$

where γ is simple shear strain and λ is the maximum peak of the reflected spectrum. The results from our model of shear strain are shown in Figure 7b (solid line). To demonstrate the effect of shear strain, a diffraction nanopattern perpendicular to

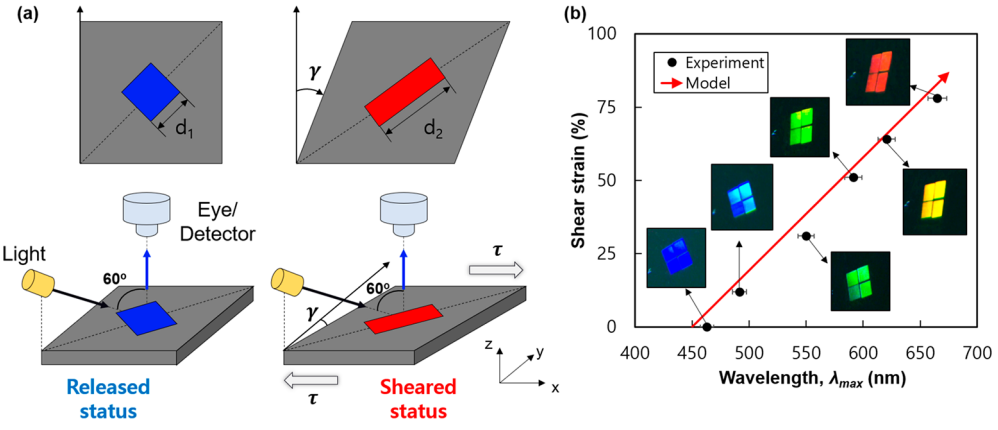

Figure 7. Shear strain sensing of the structural color-based strain sensor. (a) Working principle of the shear strain-sensing mechanism; the diffraction grating nanopatterns are placed in a diagonal direction with a pattern distance of 520 nm. (b) CCD color images and the measured maximum shear strain, compared with a theoretical model.

https://dx.doi.org/10.1021/acsnano.9b08953
ACS Nano 2020, 14, 5392−5399

the diagonal direction of a square was fabricated on the surface of a PDMS substrate. First of all, the incident and reflective angle of the diffraction structure and diffraction order are fixed according to the diffraction equation. During a simple shear strain deformation, the sample will rotate due to normal strain along the *x*-axis (Figure 7a). To overcome this phenomenon, we designed an incident white light source that can illuminate along the diagonal direction of the diffraction nanostructure arrays (see Supporting Information Figure S7). Shear strain can be measured as the incident light rotates along the diagonal direction of the diffraction array on the XY plane. As shown in Figure 7b, dark-field CCD color images were captured, and diffraction peaks measured, on application of shear stress. When the sample was illuminated with white light during stretching, the color of the shear strain sensor shifted from blue (spectral peak: 450 nm) to red (675 nm) for a shear strain range from 0% to 78%. Measured shear strains of 12%, 31%, 51%, and 64% gave the colors light blue (495 nm), dark green (540 nm), light green (585 nm), and orange (630 nm), respectively. The experimental results and theoretical model agree well, and the small variations between the measured results and the theoretical model could be due to friction while holding the sample and to normal tensile strain during the shear strain deformation.

CONCLUSION

In summary, we demonstrated the concept of, and obtained experimental results for, a stretchable, structural color-based, wireless strain sensor that can measure normal and shear strains by color change. The main purpose of this research is applying a simple and cost-effective manufacturing process to fabricate a large stretchable color-based strain sensor and its various strain-sensing mechanisms. The fundamental of plasmonic structures is based on metal nanostructure arrays on a stretchable substrate, which requires multiple manufacturing steps because of two or more different materials such as metals and elastomers and so on. Therefore, it has adhesion issues between different materials. In this research, we simply used a one-body diffractive nanostructure array, only PDMS, mixed with dark silicon pigment to implement a stretchable color-based strain sensor. Therefore, the structure presented in this study has the advantage of being more stable against fractures due to friction or external impacts compared to the plasmonic structures. In addition, because of its one-body structure, the diffractive color-based strain sensor is highly stable during the color change, which is thus highly repeatable. The strain sensor can achieve changes to all visible colors by mechanical stretching. Using different diffraction nanopatterns, we developed a large, stretchable, tensile strain sensor that can measure strain up to 100%. Moreover, due to the asymmetric 2-D diffracting pattern design, biaxial strain measurement is also possible. The structural color-based, shear strain sensor has been demonstrated using our design. The incident and reflective or collective angles for the light can be solved by designing a light guide system to guide the light pass through only in the designated direction to avoid errors. Importantly, by application of the three strain-sensing modes introduced herein, inhomogeneous plane strain can be measured using our wireless, color-based strain sensor. The developed sensor can be applied to soft robotics, structural monitoring, and wearable devices, as well as to active color filters, displays, and camouflage.

EXPERIMENTAL SECTION

Fabrication of the Diffraction-Based Structural Color Sensor. To fabricate a mold for a diffraction nanopattern, ion beam patterning was applied to a silicon substrate using a focused ion beam system (COBRA FIB; Orsay Physics, France) at an acceleration voltage of 30 keV with an ion beam current of 300 pA. The diffracting nanohole pattern of the corn shapes was designed as a 150 × 150 μm^2 square. Then, the nanopatterned silicon mold was embedded into a prepared acrylic mold for a thermal nanoimprinting process. A PDMS film with a thickness of ~2 mm was prepared by mixing the base and curing agent of a commercial product (Sylgard 184; Dow Corning, USA) with a weight ratio of 10:1; then, a commercial black silicone pigment and PDMS solution were mixed at a weight ratio of 1:100. The prepared mixture was then degassed and poured into the mold, to thermally imprint nanopatterns onto the PDMS substrate, and cured for 2 h at 80 °C. The PDMS substrate was demolded from the acrylic mold after the curing, thus completing the fabrication of a nanopatterned, stretchable, diffractive device.

Optical Measurement. To measure optical properties during diffraction, a self-built dark-field optical microscopy system was produced (Figure S1). The diffraction images were captured using a CCD camera (acA1920-155uc; Basler Ace, Germany) assembled in the microscopy system with a 5×, 0.15 NA objective lens (MPlanFL N; Olympus, Japan), and the reflected spectra were measured using a FLAME-S-VIS-NIR spectrometer (Ocean Optics, USA), measuring wavelengths from 400 to 700 nm. The incident angle of the white illumination was set to 60°, and the reflected image was captured along the normal direction.

ASSOCIATED CONTENT

Supporting Information

The Supporting Information is available free of charge at https://pubs.acs.org/doi/10.1021/acsnano.9b08953.

Optical measurement setup; theoretical calculation of strain−wavelength model; light scattering effect; tensile test; shear strain design and model; shear strain optical measurement; diffraction efficiency in the *y*-direction of the biaxial strain sensor; comparison of strain-responsive structural colors and results in this research (PDF)

AUTHOR INFORMATION

Corresponding Author

Sung-Hoon Ahn − *Institute of Advanced Machines and Design and Department of Mechanical and Aerospace Engineering, Seoul National University, Seoul 08826, Republic of Korea;* orcid.org/0000-0002-1548-2394; Email: ahnsh@snu.ac.kr

Authors

Ying-Jun Quan − *Institute of Advanced Machines and Design, Seoul National University, Seoul 08826, Republic of Korea;* orcid.org/0000-0001-7354-4736

Young-Gyun Kim − *Department of Mechanical and Aerospace Engineering, Seoul National University, Seoul 08826, Republic of Korea*

Min-Soo Kim − *Soft Robotics Research Center, Seoul National University, Seoul 08826, Republic of Korea*

Soo-Hong Min − *Department of Mechanical and Aerospace Engineering, Seoul National University, Seoul 08826, Republic of Korea*

Complete contact information is available at: https://pubs.acs.org/10.1021/acsnano.9b08953

Notes

The authors declare no competing financial interest.

https://dx.doi.org/10.1021/acsnano.9b08953
ACS Nano 2020, 14, 5392−5399

ACKNOWLEDGMENTS

This work was supported by the National Research Foundation of Korea (NRF) grant funded by the Korea Government (MSIT) (No. NRF-2018R1A2A1A13078704) and the Basic Research Lab Program (No. NRF-2018R1A4A1059976), Institute of Engineering Research, Seoul National University (SNU).

REFERENCES

(1) Rus, D.; Tolley, M. T. Design, Fabrication and Control of Soft Robots. *Nature* **2015**, *521*, 467.
(2) Mengüç, Y.; Park, Y.-L.; Pei, H.; Vogt, D.; Aubin, P. M.; Winchell, E.; Fluke, L.; Stirling, L.; Wood, R. J.; Walsh, C. J. Wearable Soft Sensing Suit for Human Gait Measurement. *Int. J. Robot. Res.* **2014**, *33*, 1748−1764.
(3) Yeo, J. C.; Yap, H. K.; Xi, W.; Wang, Z.; Yeow, C. H.; Lim, C. T. Flexible and Stretchable Strain Sensing Actuator for Wearable Soft Robotic Applications. *Adv. Mater. Technol.* **2016**, *1*, 1600018.
(4) Wang, S.; Xiao, P.; Liang, Y.; Zhang, J.; Huang, Y.; Wu, S.; Kuo, S.-W.; Chen, T. Network Cracks-Based Wearable Strain Sensors for Subtle and Large Strain Detection of Human Motions. *J. Mater. Chem. C* **2018**, *6*, 5140−5147.
(5) Kim, K.; Yun, K.-S. Stretchable Power-Generating Sensor Array in Textile Structure Using Piezoelectric Functional Threads with Hemispherical Dome Structures. *Int. J. Precis. Eng. Manuf.-Green Technol.* **2019**, *6*, 699−710.
(6) Frutiger, A.; Muth, J. T.; Vogt, D. M.; Mengüç, Y.; Campo, A.; Valentine, A. D.; Walsh, C. J.; Lewis, J. A. Capacitive Soft Strain Sensors *via* Multicore−Shell Fiber Printing. *Adv. Mater.* **2015**, *27*, 2440−2446.
(7) Chossat, J.-B.; Park, Y.-L.; Wood, R. J.; Duchaine, V. A Soft Strain Sensor Based on Ionic and Metal Liquids. *IEEE Sens. J.* **2013**, *13*, 3405−3414.
(8) Muth, J. T.; Vogt, D. M.; Truby, R. L.; Mengüç, Y.; Kolesky, D. B.; Wood, R. J.; Lewis, J. A. Embedded 3D Printing of Strain Sensors within Highly Stretchable Elastomers. *Adv. Mater.* **2014**, *26*, 6307−6312.
(9) Pang, C.; Lee, G.-Y.; Kim, T. -i.; Kim, S. M.; Kim, H. N.; Ahn, S.-H.; Suh, K.-Y. A Flexible and Highly Sensitive Strain-Gauge Sensor Using Reversible Interlocking of Nanofibres. *Nat. Mater.* **2012**, *11*, 795.
(10) Gao, Y.; Huang, C.; Hao, C.; Sun, S.; Zhang, L.; Zhang, C.; Duan, Z.; Wang, K.; Jin, Z.; Zhang, N. Lead Halide Perovskite Nanostructures for Dynamic Color Display. *ACS Nano* **2018**, *12*, 8847−8854.
(11) Hu, D.; Lu, Y.; Cao, Y.; Zhang, Y.; Xu, Y.; Li, W.; Gao, F.; Cai, B.; Guan, B.-O.; Qiu, C.-W. Laser-Splashed Three-Dimensional Plasmonic Nanovolcanoes for Steganography in Angular Anisotropy. *ACS Nano* **2018**, *12*, 9233−9239.
(12) Jiang, H.; Kaminska, B. Scalable Inkjet-Based Structural Color Printing by Molding Transparent Gratings on Multilayer Nanostructured Surfaces. *ACS Nano* **2018**, *12*, 3112−3125.
(13) Lee, G. H.; Choi, T. M.; Kim, B.; Han, S. H.; Lee, J. M.; Kim, S.-H. Chameleon-Inspired Mechanochromic Photonic Films Composed of Non-Close-Packed Colloidal Arrays. *ACS Nano* **2017**, *11*, 11350−11357.
(14) Lee, J. H.; Fan, B.; Samdin, T. D.; Monteiro, D. A.; Desai, M. S.; Scheideler, O.; Jin, H.-E.; Kim, S.; Lee, S.-W. Phage-Based Structural Color Sensors and Their Pattern Recognition Sensing System. *ACS Nano* **2017**, *11*, 3632−3641.
(15) Shang, Y.; Chen, Z.; Fu, F.; Sun, L.; Shao, C.; Jin, W.; Liu, H.; Zhao, Y. Cardiomyocyte-Driven Structural Color Actuation in Anisotropic Inverse Opals. *ACS Nano* **2019**, *13*, 796−802.
(16) Haque, M. A.; Kamita, G.; Kurokawa, T.; Tsujii, K.; Gong, J. P. Unidirectional Alignment of Lamellar Bilayer in Hydrogel: One-Dimensional Swelling, Anisotropic Modulus, and Stress/Strain Tunable Structural Color. *Adv. Mater.* **2010**, *22*, 5110−4.
(17) Song, S. C.; Ma, X. L.; Pu, M. B.; Li, X.; Liu, K. P.; Gao, P.; Zhao, Z. Y.; Wang, Y. Q.; Wang, C. T.; Luo, X. G., Actively Tunable Structural Color Rendering with Tensile Substrate. *Adv. Opt. Mater.* **2017**, *5*, 1600829.
(18) Wu, C.-S.; Tsai, P.-Y.; Wang, T.-Y.; Lin, E.-L.; Huang, Y.-C.; Chiang, Y.-W. Flexible or Robust Amorphous Photonic Crystals from Network-Forming Block Copolymers for Sensing Solvent Vapors. *Anal. Chem.* **2018**, *90*, 4847−4855.
(19) Tseng, M. L.; Yang, J.; Semmlinger, M.; Zhang, C.; Nordlander, P.; Halas, N. J. Two-Dimensional Active Tuning of an Aluminum Plasmonic Array for Full-Spectrum Response. *Nano Lett.* **2017**, *17*, 6034−6039.
(20) Chen, Y.; Duan, X.; Matuschek, M.; Zhou, Y.; Neubrech, F.; Duan, H.; Liu, N. Dynamic Color Displays Using Stepwise Cavity Resonators. *Nano Lett.* **2017**, *17*, 5555−5560.
(21) Wang, Z.; Xue, M.; Zhang, H. R.; Meng, Z. H.; Shea, K. J.; Qiu, L. L.; Ji, T. T.; Xie, T. S. Self-Assembly of a Nano Hydrogel Colloidal Array for the Sensing of Humidity. *RSC Adv.* **2018**, *8*, 9963−9969.
(22) Wang, H.; Wang, X.; Yan, C.; Zhao, H.; Zhang, J.; Santschi, C.; Martin, O. J. F. Full Color Generation Using Silver Tandem Nanodisks. *ACS Nano* **2017**, *11*, 4419−4427.
(23) Miyata, M.; Hatada, H.; Takahara, J. Full-Color Subwavelength Printing with Gap-Plasmonic Optical Antennas. *Nano Lett.* **2016**, *16*, 3166−3172.
(24) James, T. D.; Mulvaney, P.; Roberts, A. The Plasmonic Pixel: Large Area, Wide Gamut Color Reproduction Using Aluminum Nanostructures. *Nano Lett.* **2016**, *16*, 3817−23.
(25) Cheng, F.; Gao, J.; Stan, L.; Rosenmann, D.; Czaplewski, D.; Yang, X. Aluminum Plasmonic Metamaterials for Structural Color Printing. *Opt. Express* **2015**, *23*, 14552−60.
(26) Yang, Z.; Chen, Y.; Zhou, Y.; Wang, Y.; Dai, P.; Zhu, X.; Duan, H., Microscopic Interference Full-Color Printing Using Grayscale-Patterned Fabry−Perot Resonance Cavities. *Adv. Opt. Mater.* **2017**, *5*, 1700029.
(27) Shrestha, V. R.; Lee, S. S.; Kim, E. S.; Choi, D. Y. Aluminum Plasmonics Based Highly Transmissive Polarization-Independent Subtractive Color Filters Exploiting a Nanopatch Array. *Nano Lett.* **2014**, *14*, 6672−8.
(28) Ye, M.; Sun, L.; Hu, X.; Shi, B.; Zeng, B.; Wang, L.; Zhao, J.; Yang, S.; Tai, R.; Fecht, H. J.; Jiang, J. Z.; Zhang, D. X. Angle-Insensitive Plasmonic Color Filters with Randomly Distributed Silver Nanodisks. *Opt. Lett.* **2015**, *40*, 4979−82.
(29) Walls, K.; Chen, Q.; Collins, S.; Cumming, D. R. S.; Drysdale, T. D. Automated Design, Fabrication, and Characterization of Color Matching Plasmonic Filters. *IEEE Photonics Technol. Lett.* **2012**, *24*, 602−604.
(30) Park, T. H.; Yu, S.; Cho, S. H.; Kang, H. S.; Kim, Y.; Kim, M. J.; Eoh, H.; Park, C.; Jeong, B.; Lee, S. W. Block Copolymer Structural Color Strain Sensor. *NPG Asia Mater.* **2018**, *10*, 328.
(31) Kim, S.; Han, S.; Koh, Y.; Lee, H.; Lee, W. Colorimetric Humidity Sensor Using Inverse Opal Photonic Gel in Hydrophilic Ionic Liquid. *Sensors* **2018**, *18*, 1357.
(32) Howell, I. R.; Li, C.; Colella, N. S.; Ito, K.; Watkins, J. J. Strain-Tunable One Dimensional Photonic Crystals Based on Zirconium Dioxide/Slide-Ring Elastomer Nanocomposites for Mechanochromic Sensing. *ACS Appl. Mater. Interfaces* **2015**, *7*, 3641−6.
(33) Gao, L.; Zhang, Y.; Zhang, H.; Doshay, S.; Xie, X.; Luo, H.; Shah, D.; Shi, Y.; Xu, S.; Fang, H. Optics and Nonlinear Buckling Mechanics in Large-Area, Highly Stretchable Arrays of Plasmonic Nanostructures. *ACS Nano* **2015**, *9*, 5968−5975.
(34) Gutruf, P.; Zou, C.; Withayachumnankul, W.; Bhaskaran, M.; Sriram, S.; Fumeaux, C. Mechanically Tunable Dielectric Resonator Metasurfaces at Visible Frequencies. *ACS Nano* **2016**, *10*, 133.
(35) Lütolf, F.; Casari, D.; Gallinet, B. Low-Cost and Large-Area Strain Sensors Based on Plasmonic Fano Resonances. *Adv. Opt. Mater.* **2016**, *4*, 715−721.
(36) Cho, H.; Han, S.; Kwon, J.; Jung, J.; Kim, H.-J.; Kim, H.; Eom, H.; Hong, S.; Ko, S. H. Self-Assembled Stretchable Photonic Crystal for a Tunable Color Filter. *Opt. Lett.* **2018**, *43*, 3501−3504.

https://dx.doi.org/10.1021/acsnano.9b08953
ACS Nano 2020, 14, 5392−5399

(37) Ahn, S. H.; Yoon, H. S.; Jang, K. H.; Kim, E. S.; Lee, H. T.; Lee, G. Y.; Kim, C. S.; Cha, S. W. Nanoscale 3D Printing Process Using Aerodynamically Focused Nanoparticle (AFN) Printing, Micro-Machining, and Focused Ion Beam (FIB). *CIRP Ann.* **2015**, *64*, 523−526.
(38) Quan, Y.-J.; Kim, M.-S.; Kim, Y.; Ahn, S.-H. Colour-Tunable 50% Strain Sensor Using Surface-Nanopatterning of Soft Materials *via* Nanoimprinting with Focused Ion Beam Milling Process. *CIRP Ann.* **2019**, *68*, 595−598.
(39) Schubert, B. E.; Floreano, D. Variable Stiffness Material Based on Rigid Low-Melting-Point-Alloy Microstructures Embedded in Soft Poly (Dimethylsiloxane)(PDMS). *RSC Adv.* **2013**, *3*, 24671−24679.
(40) Zhang, D.; Zhang, K.; Wang, Y.; Wang, Y.; Yang, Y. Thermoelectric Effect Induced Electricity in Stretchable Graphene-Polymer Nanocomposites for Ultrasensitive Self-Powered Strain Sensor System. *Nano Energy* **2019**, *56*, 25−32.

https://dx.doi.org/10.1021/acsnano.9b08953
ACS Nano 2020, 14, 5392−5399